HHS Public Access

Author manuscript

NMR Biomed. Author manuscript; available in PMC 2018 April 01.

Published in final edited form as:

NMR Biomed. 2017 April ; 30(4): . doi:10.1002/nbm.3489.

Regionally progressive accumulation of iron in Parkinson's disease as measured by quantitative susceptibility mapping

Xiaojun Guan[1], **Min Xuan**[1], **Quanquan Gu**[1], **Peiyu Huang**[1], **Chunlei Liu**[3,4], **Nian Wang**[3], **Xiaojun Xu**[1], **Wei Luo**[2], and **Minming Zhang**[1,*]

[1]Department of Radiology, the Second Affiliated Hospital, Zhejiang University School of Medicine, Hangzhou, China

[2]Department of Neurology, the Second Affiliated Hospital, Zhejiang University School of Medicine, Hangzhou, China

[3]Brain Imaging and Analysis Center, Duke University School of Medicine, Durham, North Carolina, USA

[4]Department of Radiology, Duke University School of Medicine, Durham, North Carolina, USA

Abstract

The progression of Parkinson's disease (PD) seems to vary according to the disease stage, which greatly influences the management of PD patients. However, the underlying mechanism of progression in PD remains unclear. This study was designed to explore the progressive pattern of iron accumulation at different stages in PD patients. Sixty right-handed PD patients and 40 normal controls were recruited. According to the disease stage, 45 patients with Hoehn-Yahr stage ≤2.5 and 15 patients with Hoehn-Yahr stage ≥3 were grouped into early-stage PD (EPD) and late-stage PD (LPD) groups, respectively. The iron content in the cardinal subcortical nuclei covering the cerebrum, cerebellum and midbrain was measured using quantitative susceptibility mapping (QSM). The substantia nigra pars compacta (SNc) showed significantly increased QSM values in the EPD patients compared with the controls. In the LPD patients, while the SNc continued to show increased QSM values compared with the controls and EPD patients, the regions showing increased QSM values spread to include the substantia nigra pars reticulata (SNr), red nucleus (RN) and globus pallidus (GP). Our data also indicated that iron deposition in the GP internal segment (GPi) was more significant than in the GP external segment. No other regions showed significant changes in QSM values among the groups. Therefore, we were able to confirm a regionally progressive pattern of iron accumulation in the different stages of PD, indicating that iron deposition in the SNc is affected exclusively in the early stages of the disease while the SNr, RN and GP, and particularly the GPi segment, become involved in advanced stages of the disease. This is a preliminary study providing objective evidence of the iron-related progression in PD.

[*]**Direct all correspondence to:** Prof. Minming Zhang, MD, PhD, Department of Radiology, The Second Affiliated Hospital, Zhejiang University School of Medicine, No.88 Jiefang Road, Shangcheng District, Hangzhou, China, 31009, Phone: 86-0571-87315255, Fax: 86-0571-8735255, zhangminming@zju.edu.cn.

Keywords

Parkinson's disease; Progression; Disease stage; iron; Quantitative susceptibility mapping

Introduction

Parkinson's disease (PD) is one of the most common neurodegenerative diseases and has a progressive evolution (1). As the disease progresses, patients with Hoehn-Yahr stage > 2.5 seem to have a significantly faster disease progression (2) and show a high incidence of balance dysfunction (3). Although these clinical manifestations greatly influence the management of PD patients at different stages, the underlying mechanism remains unclear. The principal pathogenesis of PD is the selective and progressive loss of dopaminergic neurons in the substantia nigra (SN) pars compacta (SNc) (4,5) and secondary degenerative changes in the basal ganglia (6). Cerebral iron plays an important role in physiologic functions, such as the synthesis of neurotransmitters (7). By contrast, excessive iron content would promote apoptosis of neurons due to the iron-related oxidative reaction and neurotoxicity (8–10). Therefore, exploring the changes in iron macroscopically in patients at different stages of PD would contribute to a better pathological understanding of the progression of the disease.

Various MRI techniques were used to measure iron in vivo and showed selectively increased iron content in the SNc (11–16). These findings were consistent with those of early biochemical studies (17–19). For the SN pars reticulata (SNr), the iron content did not appear to increase significantly until the disease progressed to the advanced stages (11,12,14,15,20). Studies have measured the iron content in other nuclei in addition to the SN, but the results are conflicting due to the analysis of various cohorts of patients (11,14,15,21–24). Therefore, the different disease stages may lead to conflicting data.

Regionally progressive iron deposition, including levels and spatial distribution, has been indicated in the SN, which is the main impaired region in PD (11,12,14,15,20). However, whether the iron content of the all subcortical nuclei, including the cerebrum, cerebellum and midbrain, varies according to disease stage is unknown. Therefore, we hypothesized that the level and spatial distribution of iron in these cerebral regions might differ according to the stage of PD.

Quantitative susceptibility mapping (QSM) compensates for the nonlocality of magnetic field distribution (25) and provides a robust measurement of magnetic susceptibility, which is significantly correlated with the brain's iron content (26–28). In this study, we utilized QSM to investigate the cerebral iron content in the cerebrum, midbrain, and cerebellum in early- and advanced-stage PD patients. We aimed to explore the underlying differences in the level and spatial distribution of iron at different stages of PD and to explain the potential progressive pattern of iron accumulation. In addition, in order to test the robust measurement of iron by QSM, R2* was calculated afterwards.

2. Materials and methods

2.1. Subjects

Sixty right-handed PD patients with a mean age of 57.1 ± 8.2 years and 40 gender- and age-matched healthy controls with a mean age of 56.6 ± 9.9 years were recruited from the Department of Neurology, the Second Affiliated Hospital of Zhejiang University School of Medicine. All PD patients were further subdivided into 2 groups according to their severity of motor impairment. Finally, 45 patients with Hoehn-Yahr stage ≤2.5 were grouped into the early-stage PD (EPD) group and 15 patients with Hoehn-Yahr stage ≥3 were grouped into the late-stage PD (LPD) group.

PD was diagnosed by a neurologist (Dr. Luo) according to the UK PD Brain Bank criteria. The exclusion criteria included other neurologic or psychiatric disorders, brain trauma, and general exclusion criteria for MR scanning. The Unified Parkinson's Disease Rating Scale (UPDRS) and the Mini-Mental State Examination (MMSE) scores and the disease duration were recorded for all patients. No patients were cognitively impaired according to the MMSE. Thirty-nine patients were taking medication with a good response. Anti-parkinsonian medication was terminated at least 12 h prior to the clinical assessments and image scanning. Normal subjects recruited for the present study were excluded if they had a history of neurologic or psychiatric disorders or brain trauma. Table 1 shows the demographic characteristics of the participants.

All subjects provided informed consent to participate in the study, which was approved by the Medical Ethic Committee of the Second Affiliated Hospital, Zhejiang University School of Medicine.

2.2 MRI, QSM and R2*

The MR images were acquired using a 3.0 Tesla machine (GE Medical Systems, Signa Excite). During MRI scanning, ear plugs and foam pads were used to reduce noise and head motion. Three-dimensional, multi-echo, gradient echo images were acquired with flow-compensated, 3D-enhanced T2 star-weighted angiography sequences. Manual shimming was conducted before scanning each patient to ensure that the static magnetic field was uniform. Due to patients' parkinsonian tremors, all images were cautiously checked after scanning; if the quality was poor because of a motion artifact, the sequence was re-scanned. The typical parameters were as follows: in-plane resolution = 0.78125×0.78125; TR = 45 ms; TE = 5.0, 10.02, 15.04, 20.06, 25.08, 30.10, 35.12 and 40.14 ms; flip angle = 25°; slice thickness = 2.8 mm; slice spacing = 0 mm; bandwidth = 31.25 Hz/pixel; and matrix size = 240 × 240. The total scan time was 3 min 30 s.

A computer cluster using STI Suite software (Duke University) processed phase images retrieved in DICOM format from the MRI scanner (29,30). First, the phase images were unwrapped using the Laplacian method, which relies only on the sine and cosine functions of the phase angle (26,31). Next, due to the large background phase overwhelming the tissue phase contrast in the unwrapped phase, the V-SHARP method, with a spherical mean radius increasing from 0.6 mm at the boundary of the brain to 25 mm toward the center of the brain, was used to remove the background phase (26,32). The resulting tissue phase was then

used to compute the susceptibility maps using an improved LSQR algorithm (29). The quantitative susceptibility assessments of various deep nuclei regions were made by using the susceptibility of cerebrospinal fluid as a reference (26,31). It has recently been shown that the iLSQR algorithm provides an unbiased estimate of tissue susceptibility with negligible streaking artifacts, in contrast to multi-orientation QSM reconstruction (29).

R2* images were processed using the multi-gradient-echo data with fitting of the monoexponential equation. All of these steps were performed in MATLAB (2009b) using home-made program.

2.3 Region of interest (ROI) determination

ITK-SNAP (www.itksnap.org) was used to perform manual segmentation and measure the QSM and R2* values for each nucleus. Data for each region were obtained from the entire visible slice. An experienced neuroradiologist responsible for the ROI analysis was blinded to the information about the subjects, including disease status and demographics. ROIs were drawn to cover the cerebrum, cerebellum and midbrain, including the SNr, SNc, red nucleus (RN), putamen, globus pallidus (GP), thalamus, head of caudate and dentate nucleus (Fig. 1). The SNr was identified as the band of high signal in the ventrolateral midbrain, while the region between the SNr and RN was considered to represent the SNc (11–16). Furthermore, it is well known that the SNr/GP internal (GPi) segment is a functional complex regarded as a key node in the pathophysiological changes of PD (6). A recent study revealed that QSM could accurately depict the medial medullary lamina, which is the boundary of the GPi and GP external (GPe) segments (21). Therefore, in the present study, we also delineated the subregions of the GP in our susceptibility maps and measured the QSM values in these regions (Fig. 2). To investigate the reproducibility and reliability of the QSM data, the same experienced neuroradiologist responsible for the ROI analysis again measured the total subcortical nuclei 3 months later.

2.4 Statistical analysis

All data were analyzed using IBM SPSS Statistics version 19.0. The normal distribution of data was confirmed using the one-sample Kolmogorov-Smirnov test. Differences in gender and age distribution of the three groups were compared using analysis of variance (ANOVA) for age and the Pearson chi-square test for gender. The intra-class correlation coefficients (ICCs) for the agreement between QSM measurements at the two time points were calculated. Differences in disease duration, UPDRS motor scores and MMSE scores between the two PD groups were also compared by an independent samples t-test, while the medication history was compared by the Pearson chi-square test. Regional QSM values and R2* values (the average values of the bilateral regions) were compared using ANOVA for the three groups (EPD, LPD and control) controlling for age and gender. The intergroup comparisons were performed using Bonferroni correction. Correlation analyses regarding age and gender as covariates between the regional iron content and disease severity were conducted in the PD patients. In addition, to quantify the contrast between the GPi and GPe segments for each group, paired t-tests were also performed. All tests were two-tailed ($a = 0.05$). A p-value less than 0.05 was considered to be statistically significant.

3. Results

3.1 Demographic data among the three groups

In the present study, there were no significant differences in gender ($p = 0.374$) and age ($p = 0.130$) among the controls, EPD and LPD patients. To control for the underlying cofounders, we determined that there were no statistically significant differences in the MMSE scores ($p = 0.578$) and medication history ($p = 0.639$) between the EPD and LPD patients (Table 1). It is important to note that a tendency for increased disease duration ($p = 0.078$) was observed in LPD patients, probably because PD is a progressive degenerative disorder.

3.2 Regional iron deposition at different stages using QSM

The ICCs for agreement between QSM measurements at the two time points were greater than 0.810 (95% confidence interval: 0.730–0.868), showing excellent agreement between the two measurements (for details, see Supporting Information Table S1).

The intercomparisons of QSM values among the groups in the subcortical nuclei, including the cerebrum, cerebellum and midbrain, were performed controlling for age and gender (Fig. 3). The QSM values significantly increased in the SNc for EPD patients compared with those of the normal controls ($p < 0.001$), indicating increased iron content in this region. In LPD patients, while the SNc continued to show increased QSM values compared with those of the controls and EPD patients (both $p < 0.001$), the regions showing increased QSM values spread to the SNr (LPD vs. controls, $p < 0.001$; LPD vs. EPD, $p = 0.031$); RN (LPD vs. controls, $p = 0.018$); and GP (LPD vs. controls, $p = 0.006$; LPD vs. EPD, $p = 0.004$). Interestingly, the absence of differences in QSM values in the GP ($p = 1.000$), RN ($p = 0.178$) and SNr ($p = 0.353$) between the controls and EPD patients was noted throughout our data. No other regions showed significant changes in QSM values among the controls, EPD and LPD patients.

Nevertheless, in contrast to the results of QSM, the R2* indicated that the only region showing iron deposition was the SNc in the PD groups compared with the controls (EPD vs. controls, $p < 0.031$; LPD vs. controls, $p < 0.017$) (for details, see Supporting Information Fig. S1). Therefore, by comparing these results of R2* and QSM, QSM was more sensitive in exploring the underlying alterations of iron content in the iron-rich regions, such as SNr, GP and RN between patients groups.

3.3 Correlations between clinical features and regional iron content

In the PD patients recruited for the present study, we observed that the iron content in the SNc and GP was significantly correlated with the Hoehn-Yahr stage ($r = 0.375$, $p = 0.004$; $r = 0.314$, $p = 0.016$, respectively) (Fig. 4A–B), and the former was also significantly correlated with the UPDRS motor scores ($r = 0.335$, $p = 0.010$) (Fig. 4C). However, we found no correlation between the iron content in the RN and disease severity.

3.4 GP subregions

We also observed changes in the QSM values in the internal structure of the GP (Fig. 2). First, among the groups, the QSM values in both the GPi and GPe segments significantly

increased in the LPD patients compared with the EPD patients ($p = 0.006$ and 0.017, respectively) and controls ($p = 0.006$ and 0.029, respectively), and the data also indicated that the levels of increased iron content in the GPi segments were higher than those in the GPe segments (Fig. 3). In addition, we confirmed the natural contrast in the internal structure of the GP, in which QSM values in the GPe segment were significantly higher than those in the GPi segment ($p < 0.001$) in the controls; this was also observed in the EPD patients ($p < 0.001$) (Table 2). By contrast, in the LPD patients, the initial contrast of the GPe and GPi segments was entirely absent ($p = 0.881$), providing more evidence that the iron content in the GPi segment increased more significantly than in the GPe segment (Table 2). Briefly, the iron content in the subregions of the GP, and particularly in the GPi segment, significantly increased in the LPD patients.

4. Discussion

The key finding in the present study was the regionally progressive accumulation of iron from the SNc to the SNr, RN and GP during disease progression. By focusing on the GP, we confirmed that QSM could accurately depict the internal structure of the GP. In addition, the iron content in the GPi segment increased more significantly than that in the GPe segment in LPD patients. Finally, by comparing with R2*, QSM seemed to be more sensitive in exploring the difference of iron deposition in the iron-rich regions.

4.1 Progressive iron accumulation within the SN

Compared with the normal controls, we found that EPD patients exhibited significantly elevated iron content specifically in the SNc. As the disease progressed into the late stages (LPD), iron deposition extended to the SNr. Because the SNc is the main impaired structure in PD, this region is likely to be more vulnerable to iron accumulation than other cerebral regions, and the iron content in this region was significantly correlated with disease severity. Bartzokis et al (33) reported iron deposition in both the SNc and SNr in early-onset PD patients, indicating that the time of disease onset is not the key factor that influences iron distribution within the SN. By recruiting non-demented, moderately affected PD patients, Nestrasil et al (13) and Du et al (16) also found significant iron deposition in the SNc region. Consistent with our findings, iron accumulation exclusively in the SNc was observed in EPD patients (12,14), while that in the SNr was only seen in advanced PD patients (12). These results confirm that iron deposition in the SNc, which is the relevant region in EPD patients, is a prospective biomarker indicating early- stage PD. By contrast, iron deposition in the SNr indicates a later stage of PD.

4.2 Enlarged extent of progressive iron accumulation

As the progressive iron deposition within the SN was confirmed above, we also explored the whole brain nuclei, including the cerebrum, midbrain and cerebellum, to determine the progression-related changes in iron content. In LPD patients, the elevated iron content further spread to the GP and RN compared with that in EPD patients, a finding that corresponded to our hypothesis. Increasing iron content in these regions would impair the behavioral function during normal aging (34). This finding may suggest that significant iron

deposition in the GP and RN might be related to severe behavioral dysfunction, which is shown in LPD patients in the present study.

Though studies have been performed extensively on the changes of iron content in PD, this progressive iron accumulation in the different stages has not yet been reported. Iron deposition in the GP was not consistently evaluated in previously published studies (11,14,21,22). Although most studies recruiting general PD patients reported no significant change in the iron content in the GP (11,14,21), Ye et al (22) observed significant iron deposition in the GP in a long-disease-duration cohort similar to our LPD patients, and the iron content significantly correlated with disease severity. These results indicate that iron deposition in the GP might be influenced by disease stage. As a result, our data showed iron deposition in this region exclusively in the LPD patients, and the significant correlation between the Hoehn-Yahr stage and GP iron content further supported that hypothesis.

Regarding the RN, in the present study, the iron content did not significantly change in our EPD patients, as shown in previously published studies (12,14), while the iron content in the same region significantly increased in the LPD patients compared with the controls. Although this result might seem unexpected at first, it may very well reflect the function of the cerebello-thalamo-cortical circuit. Due to the presence of basal ganglia dysfunction in PD patients, the RN might increase its function to fulfill cerebellar compensation (35). Therefore, we speculate that iron deposition in this region exclusively in patients with severe motor impairment (LPD patients) probably indicates significantly increased cerebellar compensation. In addition, the absence of significant iron deposition in the EPD patients indicates that basal ganglia dysfunction in these patients might not significantly activate cerebellar compensation. However, a recently published PD study found iron deposition in this region, especially in early patients (36), which differed from both the findings in previous studies (11,12,14) and the present findings. It is difficult to explain the reasons underlying this inconsistency, but the results in the EPD patients in our study are supported by the work of others (11,12,14). In addition, Wang et al (12) did not observe this pattern of iron deposition in their study, which involved a small sample (n=7) of late-stage patients and used phase imaging. The enlarged sample size in the present study and the robust measurements using QSM could probably explain the inconsistency. Therefore, this finding indicates a potential pathological change in the progression in PD. However, for further implications of this finding, the iron content in this region in the LPD patients should be confirmed in future studies.

4.3 Special insight into the internal structure of the GP

Overactivity of the SNr/GPi complex plays an important pathophysiologic role in the manifestation of motor impairment in PD (6). We found that the iron content in the GPi and GPe segments significantly increased exclusively in the LPD patients, similar to what was found in the SNr, and the iron content in the GPi segment increased more significantly than in the GPe segment. In a recent study, Ide et al (21) demonstrated the usefulness of QSM in identifying the internal structure of the GP in PD patients, and that result was supported by our data of EPD patients. However, there were also conflicting results in these regions. By using T2 mapping, Kosta et al (15) found significantly decreased T2 values in the GPe

segment, indicating increased iron content in this region, while the T2 values in the GPi segment did not significantly change. Griffiths et al (24,37) reported significantly increased iron content in the GPe segment but decreased iron content in the GPi segment in the brains of six deceased PD patients. There are several possible reasons for these conflicting results. First, the patients without a classification of disease stage would degrade the statistical significance for certain regions, and technologically, increased iron content with decreased T2 values would be compromised by the increased water content in the diseased tissues. Therefore, QSM could provide a robust measurement of the iron content independent of water influence in the present study. Second, a postmortem study is identified as the gold standard; however, the sample size (n = 6) in the previous study (24,37) was rather small. Taken together, our data showed that the iron content in the GP varies according to the internal structures and disease stage. The GPi segment, as a node of the SNr/GPi complex, which showed a similar iron deposition to the SNr, is probably the main involved subregion within the GP in LPD patients. However, it remains unclear whether iron deposition in these regions results in an oxidative reaction or in secondary changes in neuronal physiology, such as extrametabolic load (37,38). Through this preliminary study using QSM, further pathophysiologic studies focusing on the influences of iron content in the GP, and particularly in the GPi segment, in LPD patients are necessary.

4.4 Different patterns of iron deposition measured by QSM and R2*

The only region showing significantly increased R2* values was the SNc in the PD groups compared with the controls in the current study, which was supported by previous studies (14,16). Compared with R2* which has lower contrast-to-noise ratio, QSM is a more robust measurement for quantifying iron content (16,36) and compensating for the nonlocality of magnetic field distribution (25). That probably accounts for the different results between the two technologies. In addition, our finding that QSM shows extra iron deposition in the GP, SNr and RN in the LPD patients indicates a notion that QSM could provide more quantitative information of iron deposition in the iron-rich regions.

4.5 Limitations

In the present study, some limitations should be noted. First, the diagnosis of PD patients lacked pathological confirmation. However, all patients included in the present study were assessed and diagnosed through longitudinal evaluations. Any patients who were diagnosed longitudinally with an atypical parkinsonian disease, such as progressive supranuclear palsy or multiple system atrophy, were excluded before the current analysis. Second, the sample size of the LPD patients was relatively small, and the results should therefore be interpreted cautiously. However, compared with the previous study (12), we have enlarged sample size and measured the iron content more robustly using QSM. Therefore, repeated studies with larger samples should be carried out in the future.

4.6 Conclusion

The quantitative assessment of QSM was demonstrated to be effective for measuring iron content in the cerebrum, midbrain and cerebellum to explore the underlying pathologic changes of PD. Here, we confirmed the regionally progressive pattern of iron accumulation in the different stages of PD patients, indicating that iron deposition in the SNc is affected

exclusively in early stages of the disease, while the SNr, RN and GP, and particularly the GPi segment, become involved in advanced stages of PD. This is a preliminary study exploring the potential pathogenesis of PD at different stages and providing objective evidence of the iron-related progression throughout the brain in PD.

Supplementary Material

Refer to Web version on PubMed Central for supplementary material.

Acknowledgments

Our study was supported by the twelfth Five-year Plan for National Science and Technology Supporting Program of China (Grant No. 2012BAI10B04); the National Natural Science Foundation of China (Grant Nos. 81371519 and 81301190). C.L. is partially supported by the US National Institutes of Health through grant NINDS R01NS079653.

Abbreviations used

PD	Parkinson’s disease
QSM	quantitative susceptibility mapping
EPD	early-stage Parkinson’s disease
LPD	late-stage Parkinson’s disease
UPDRS	Unified Parkinson's Disease Rating Scale
MMSE	Mini-Mental State Examination
ANOVA	analysis of variance
SNc	substantia niga pars compacta
SNr	substantia niga pars reticulata
GP	globus pallidus
GPi	globus pallidus internal
GPe	globus pallidus external
RN	red nucleus

References

1. Lees AJ, Hardy J, Revesz T. Parkinson's disease. Lancet. 2009; 373(9680):2055–2066. [PubMed: 19524782]
2. Zhao YJ, Wee HL, Chan Y, Seah SH, Au WL, Lau PN, Pica EC, Li SC, Luo N, Tan LCS. Progression of Parkinson's disease as evaluated by Hoehn and Yahr stage transition times. Mov. Disord. 2010; 25(6):710–716. [PubMed: 20213822]
3. Latt MD, Lord SR, Morris JGL, Fung VSC. Clinical and physiological assessments for elucidating falls risk in Parkinson's disease. Mov. Disord. 2009; 24(9):1280–1289. [PubMed: 19425059]

4. Damier P. The substantia nigra of the human brain. II. Patterns of loss of dopamine-containing neurons in Parkinson's disease. Brain. 1999; 122(8):1437–1448. [PubMed: 10430830]
5. Fearnley JM, Lees AJ. Ageing and Parkinson's disease: substantia nigra regional selectivity. Brain. 1991; 114(5):2283–2301. [PubMed: 1933245]
6. Obeso JA, Rodriguez-Oroz MC, Rodriguez M, Lanciego JL, Artieda J, Gonzalo N, Olanow CW. Pathophysiology of the basal ganglia in Parkinson's disease. Trends Neurosci. 2000; 23(10 Suppl):S8–S19. [PubMed: 11052215]
7. Beard JL, Connor JR, Jones BC. Iron in the brain. Nutr. Rev. 1993; 51(6):157–170. [PubMed: 8371846]
8. Ward RJ, Dexter DT, Crichton RR. Neurodegenerative diseases and therapeutic strategies using iron chelators. J. Trace Elem. Med. Biol. 2015; 31:267–273. [PubMed: 25716300]
9. You LH, Li F, Wang L, Zhao SE, Wang SM, Zhang LL, Zhang LH, Duan XL, Yu P, Chang YZ. Brain iron accumulation exacerbates the pathogenesis of MPTP-induced Parkinson's disease. Neuroscience. 2015; 284:234–246. [PubMed: 25301748]
10. Gaasch JA, Lockman PR, Geldenhuys WJ, Allen DD, Van der Schyf CJ. Brain iron toxicity: differential responses of astrocytes, neurons, and endothelial cells. Neurochem. Res. 2007; 32(7): 1196–1208. [PubMed: 17404839]
11. Rossi M, Ruottinen H, Soimakallio S, Elovaara I, Dastidar P. Clinical MRI for iron detection in Parkinson's disease. Clin. Imaging. 2013; 37(4):631–636. [PubMed: 23522789]
12. Wang C, Fan G, Xu K, Wang S. Quantitative assessment of iron deposition in the midbrain using 3D-enhanced T2 star weighted angiography (ESWAN): a preliminary cross-sectional study of 20 Parkinson's disease patients. Magn. Reson. Imaging. 2013; 31(7):1068–1073. [PubMed: 23746648]
13. Nestrasil I, Michaeli S, Liimatainen T, Rydeen CE, Kotz CM, Nixon JP, Hanson T, Tuite PJ. T1rho and T2rho MRI in the evaluation of Parkinson's disease. J. Neurol. 2010; 257(6):964–968. [PubMed: 20058018]
14. Martin WRW, Wieler M, Gee M. Midbrain iron content in early Parkinson disease: a potential biomarker of disease status. Neurol. 2008; 70(16 Pt):1411–1417.
15. Kosta P, Argyropoulou MI, Markoula S, Konitsiotis S. MRI evaluation of the basal ganglia size and iron content in patients with Parkinson's disease. J. Neurol. 2006; 253(1):26–32. [PubMed: 15981079]
16. Du G, Liu T, Lewis MM, Kong L, Wang Y, Connor J, Mailman RB, Huang X. Quantitative susceptibility mapping of the midbrain in Parkinson's disease. Mov. Disord. 2015
17. Sofic E, Paulus W, Jellinger K, Riederer P, Youdim MBH. Selective increase of iron in substantia nigra zona compacta of parkinsonian brains. J. Neurochem. 1991; 56(3):978–982. [PubMed: 1704426]
18. Jellinger K, Paulus W, Grundke-Iqbal I, Riederer P, Youdim MBH. Brain iron and ferritin in Parkinson's and Alzheimer's diseases. J. Neural Transm. Park. Dis. Dement. Sect. 1990; 2(4):327–340. [PubMed: 2078310]
19. Dexter DT, Carayon A, Javoy-agid F, Agid Y, Wells FR, Daniel SE, Lees AJ, Jenner P, Marsden CD. Alterations in the levels of iron, ferritin and other trace metals in Parkinson's disease and other neurodegenerative diseases affecting the basal ganglia. Brain. 1991; 114(4):1953–1975. [PubMed: 1832073]
20. Du G, Lewis MM, Sen S, Wang J, Shaffer ML, Styner M, Yang QX, Huang X. Imaging nigral pathology and clinical progression in Parkinson's disease. Mov. Disord. 2012; 27(13):1636–1643. [PubMed: 23008179]
21. Ide S, Kakeda S, Ueda I, Watanabe K, Murakami Y, Moriya J, Ogasawara A, Futatsuya K, Sato T, Ohnari N, Okada K, Matsuyama A, Fujiwara H, Hisaoka M, Tsuji S, Liu T, Wang Y, Korogi Y. Internal structures of the globus pallidus in patients with Parkinson's disease: evaluation with quantitative susceptibility mapping (QSM). Eur. Radiol. 2015; 25(3):710–718. [PubMed: 25361824]
22. Ye FQ, Allen PS, Martin WRW. Basal ganglia iron content in Parkinson's disease measured with magnetic resonance. Mov. Disord. 1996; 11(3):243–249. [PubMed: 8723139]

23. Graham JM. Brain iron deposition in Parkinson's disease imaged using the PRIME magnetic resonance sequence. Brain. 2000; 123(12):2423–2431. [PubMed: 11099445]
24. Griffiths PD. Iron in the basal ganglia in Parkinson's disease. An in vitro study using extended X-ray absorption fine structure and cryo-electron microscopy. Brain. 1999; 122(4):667–673. [PubMed: 10219780]
25. Liu C, Li W, Tong KA, Yeom KW, Kuzminski S. Susceptibility-weighted imaging and quantitative susceptibility mapping in the brain. J. Magn. Reson. Imaging. 2015; 42(1):23–41. [PubMed: 25270052]
26. Wu B, Li W, Guidon A, Liu C. Whole brain susceptibility mapping using compressed sensing. Magn. Reson. Med. 2012; 67(1):137–147. [PubMed: 21671269]
27. Bilgic B, Pfefferbaum A, Rohlfing T, Sullivan EV, Adalsteinsson E. MRI estimates of brain iron concentration in normal aging using quantitative susceptibility mapping. Neuroimage. 2012; 59(3): 2625–2635. [PubMed: 21925274]
28. Langkammer C, Schweser F, Krebs N, Deistung A, Goessler W, Scheurer E, Sommer K, Reishofer G, Yen K, Fazekas F, Ropele S, Reichenbach JR. Quantitative susceptibility mapping (QSM) as a means to measure brain iron? A post mortem validation study. Neuroimage. 2012; 62(3):1593–1599. [PubMed: 22634862]
29. Li W, Wang N, Yu F, Han H, Cao W, Romero R, Tantiwongkosi B, Duong TQ, Liu C. A method for estimating and removing streaking artifacts in quantitative susceptibility mapping. Neuroimage. 2015; 108:111–122. [PubMed: 25536496]
30. Li W, Avram AV, Wu B, Xiao X, Liu C. Integrated Laplacian-based phase unwrapping and background phase removal for quantitative susceptibility mapping. N.M.R. Biomed. 2014; 27(2): 219–227.
31. Li W, Wu B, Liu C. Quantitative susceptibility mapping of human brain reflects spatial variation in tissue composition. Neuroimage. 2011; 55(4):1645–1656. [PubMed: 21224002]
32. Li W, Wu B, Batrachenko A, Bancroft-Wu V, Morey RA, Shashi V, Langkammer C, De Bellis MD, Ropele S, Song AW, Liu C. Differential developmental trajectories of magnetic susceptibility in human brain gray and white matter over the lifespan. Hum. Brain Mapp. 2014; 35(6):2698–2713. [PubMed: 24038837]
33. Bartzokis G, Cummings JL, Markham CH, Marmarelis PZ, Treciokas LJ, Tishler TA, Marder SR, Mintz J. MRI evaluation of brain iron in earlier-and later-onset Parkinson's disease and normal subjects. Magn. Reson. Imaging. 1999; 17(2):213–222. [PubMed: 10215476]
34. Li W, Langkammer C, Chou Y, Petrovic K, Schmidt R, Song AW, Madden DJ, Ropele S, Liu C. Association between increased magnetic susceptibility of deep gray matter nuclei and decreased motor function in healthy adults. Neuroimage. 2015; 105:45–52. [PubMed: 25315786]
35. Lewis MM, Du G, Kidacki M, Patel N, Shaffer ML, Mailman RB, Huang X. Higher iron in the red nucleus marks Parkinson's dyskinesia. Neurobiol. Aging. 2013; 34(5):1497–1503. [PubMed: 23177595]
36. He N, Ling H, Ding B, Huang J, Zhang Y, Zhang Z, Liu C, Chen K, Yan F. Region-specific disturbed iron distribution in early idiopathic Parkinson's disease measured by quantitative susceptibility mapping. Hum. Brain Mapp. 2015; 36:4407–4420. [PubMed: 26249218]
37. Griffiths PD, Crossman AR. Distribution of iron in the basal ganglia and neocortex in postmortem tissue in Parkinson's disease and Alzheimer's disease. Dementia. 1993; 4(2):61–65. [PubMed: 8358514]
38. Mash DC, Pablo J, Buck BE, Sanchez-Ramos J, Weiner WJ. Distribution and number of transferrin receptors in Parkinson's disease and in MPTP-treated mice. Exp. Neurol. 1991; 114(1):73–81. [PubMed: 1915737]

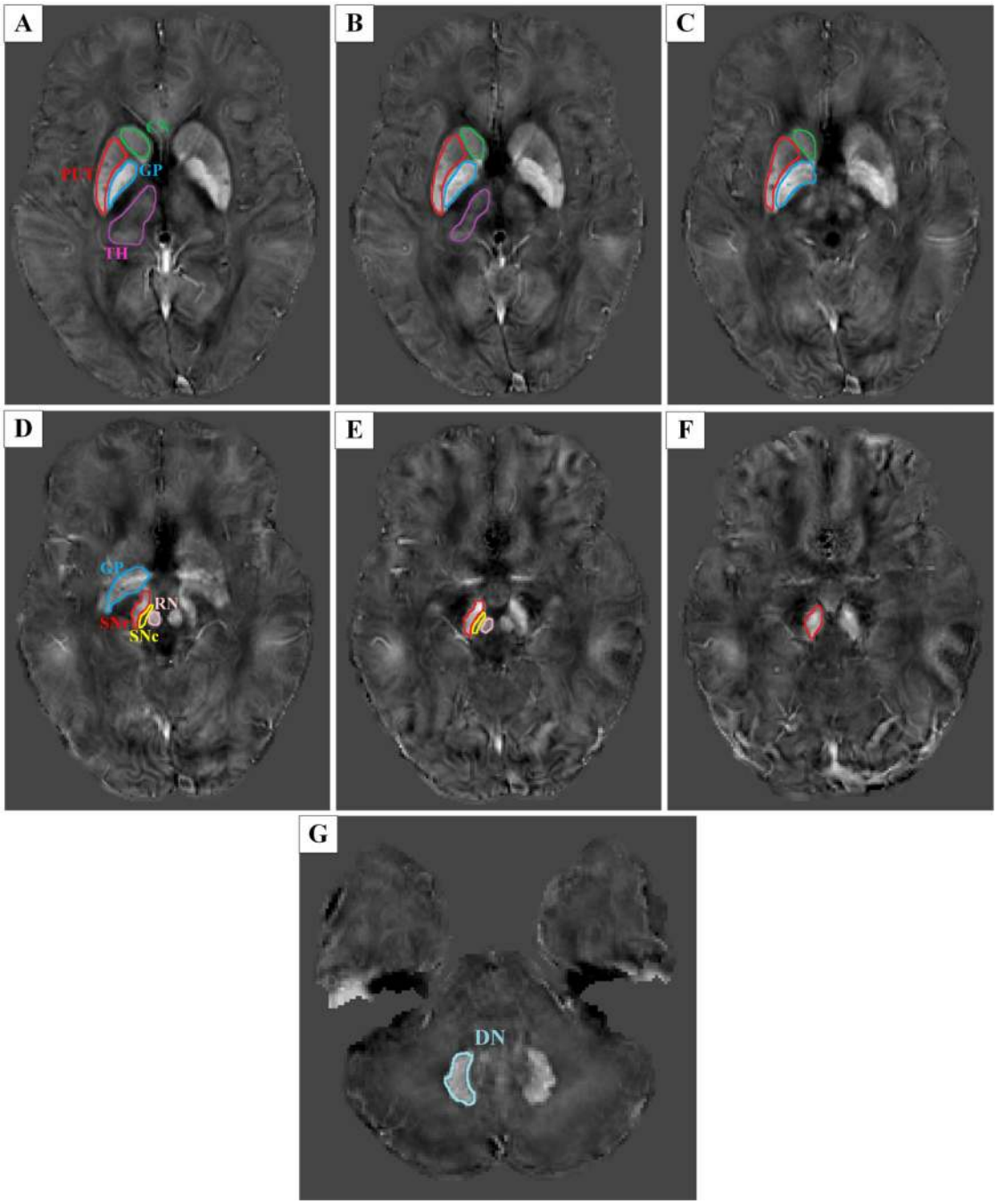

Fig. 1.

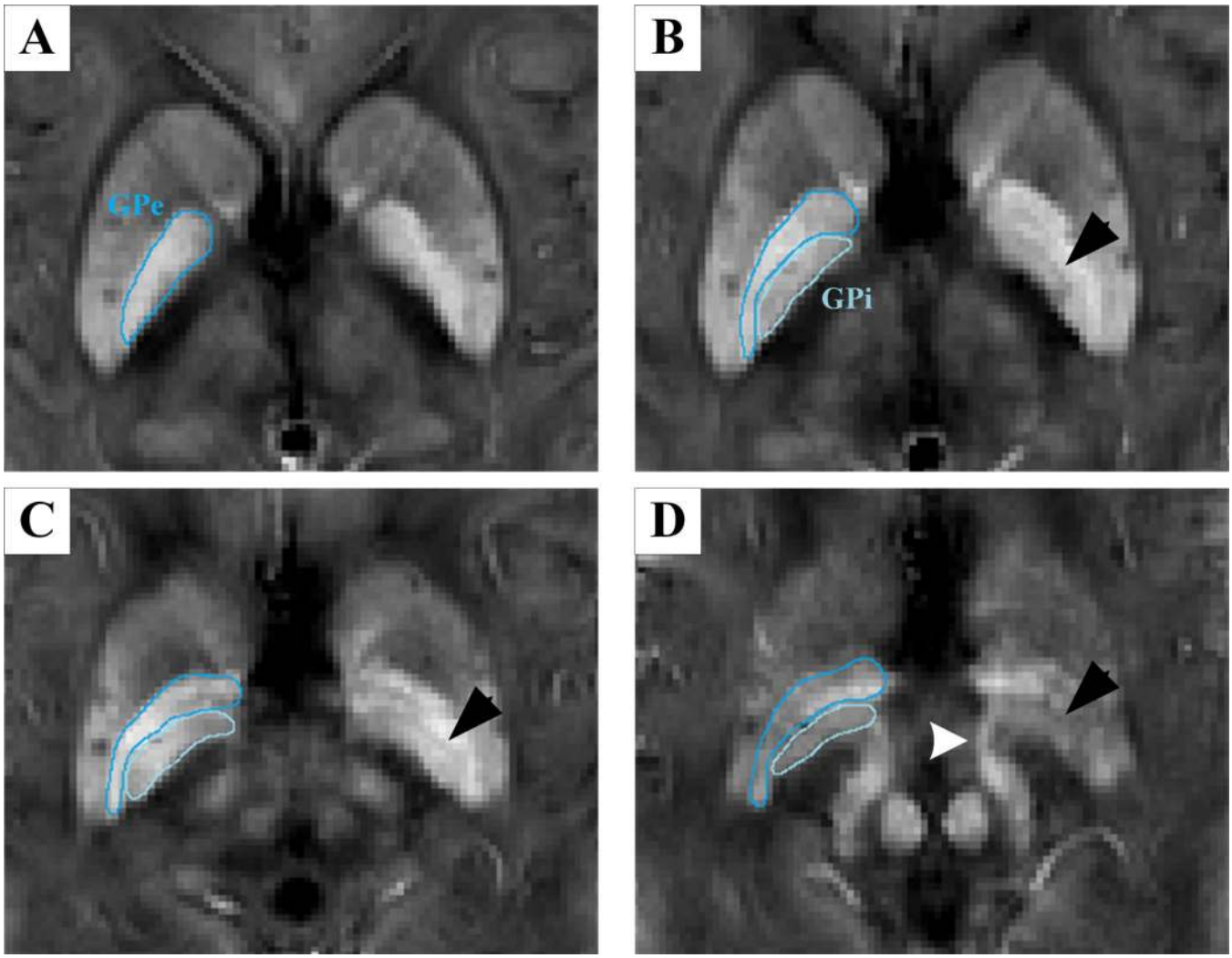

Fig. 2.

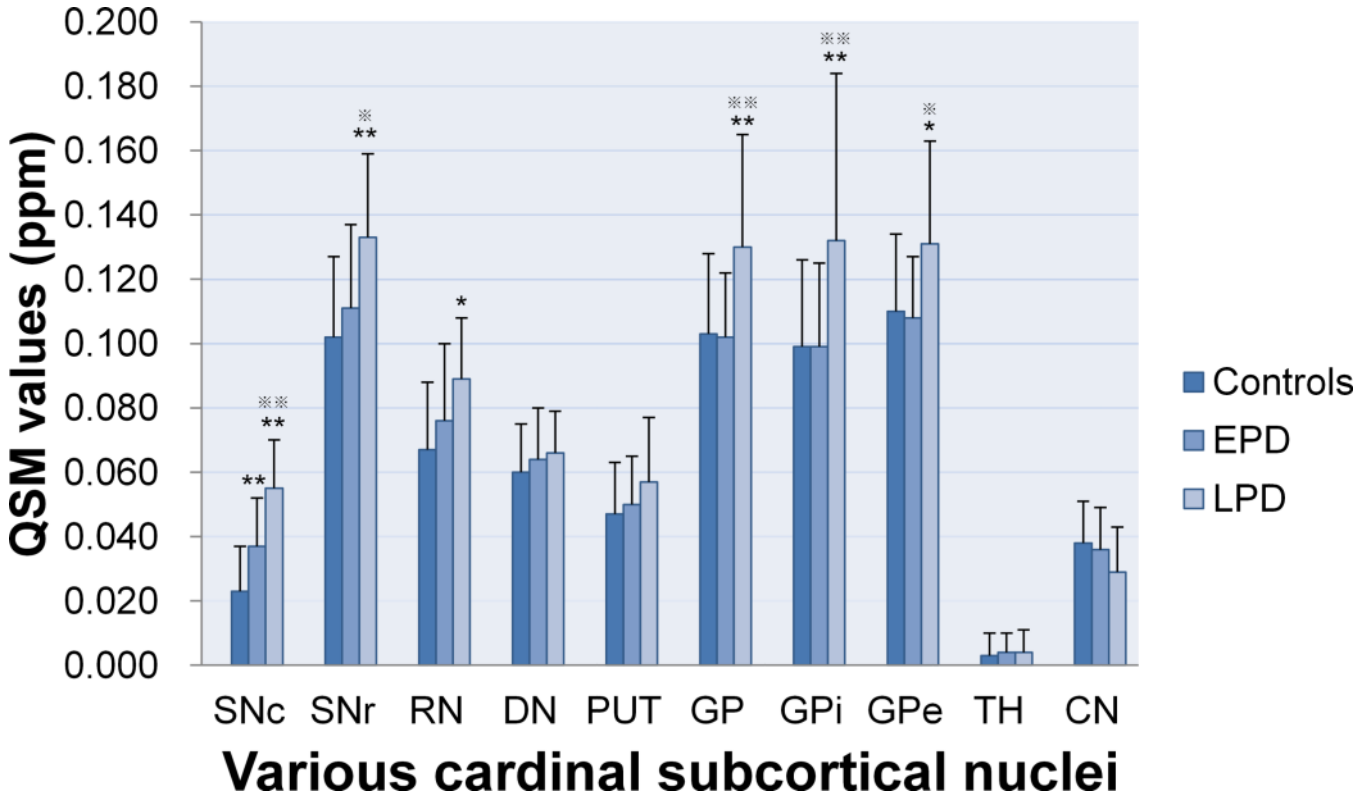

Fig. 3.

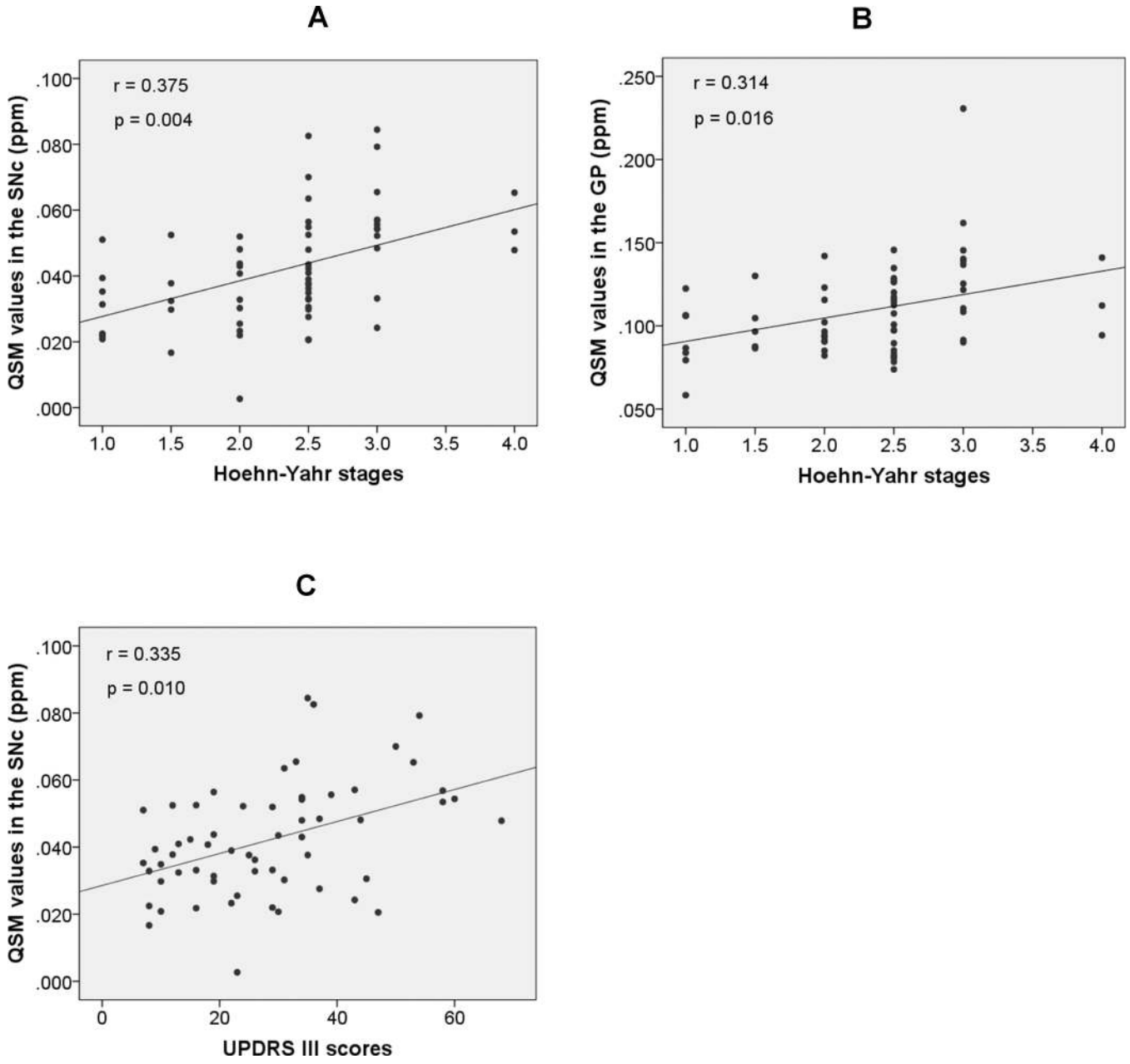

Fig. 4.

Table 1

Group demographics and clinical status

	Controls	EPD	LPD	p values
No. (male/female)	40 (19/21)	45 (21/24)	15 (10/5)	0.374
Age in years, mean ± SD	56.6 ± 9.9	55.8 ± 8.3	61.1 ± 6.7	0.130
Disease duration in years, mean ± SD	–	4.6 ± 3.7	6.7 ± 4.7	0.078
Hoehn-Yahr stages, mean ± SD	–	2.0 ± 0.6	3.2 ± 0.4	**<0.001**
UPDRS III scores, mean ± SD	–	22.8 ± 11.7	44.5 ± 13.1	**<0.001**
MMSE scores, mean ± SD	–	28.24 ± 1.8	27.7 ± 2.0	0.578
Medication (yes/no)	–	30/15	9/6	0.639

Abbreviations: EPD = early-stage Parkinson's disease; LPD = late-stage Parkinson's disease; UPDRS = Unified Parkinson's Disease Rating Scale; MMSE = Mini-Mental State Examination.

Table 2

Contrast between the GPi and GPe segments among the groups

	QSM values (ppm)			
Group	**GPe**	**GPi**	**Differences in GPe and GPi (95% confidence interval)**	**p values**
Controls	0.110 ± 0.024	0.099 ± 0.027	0.010 (−0.006 ~ 0.014)	< 0.001
EPD	0.108 ± 0.019	0.099 ± 0.026	0.009 (−0.004 ~ 0.014)	< 0.001
LPD	0.131 ± 0.032	0.132 ± 0.052	−0.001 (−0.016 ~ 0.014)	0.881

Abbreviations: EPD = early-stage Parkinson's disease; LPD = late-stage Parkinson's disease; GPe = globus pallidus external; GPi = globus pallidus internal.